Available online at www.sciencedirect.com
SCIENCE DIRECT®
C. R. Chimie 7 (2004) 395–400
COMPTES RENDUS CHIMIE

Preliminary communication / Communication

High-temperature NMR study of Al dissolution in cryolitic melts

Ioana Nuta *, Catherine Bessada, Emmanuel Veron, Guy Matzen

CNRS–CRMHT, 1D, av. de la Recherche-Scientifique, 45071 Orléans cedex 2, France

Received 17 July 2003; accepted 3 December 2003

Available online 15 April 2004

Abstract

The dissolution of aluminium in cryolitic melts is the major cause of the loss in current efficiency during the industrial process of aluminium electrolysis. These melts are corrosive and not easy to handle experimentally. Using the laser-heated device, associated with a tightly closed crucible, we have studied different compositions of the NaF–AlF_3–Al system by ^{27}Al, ^{23}Na and ^{19}F in situ NMR at 1030 °C. The samples were also characterized after rapid cooling at room temperature by MAS NMR, X-rays diffraction and microscopy in order to describe the structure of the solidified phases. ***To cite this article: I. Nuta et al., C. R. Chimie 7 (2004).***

Résumé

La dissolution de l'aluminium dans les bains cryolitiques est une des causes principales de faible rendement électrique dans le procédé d'électrolyse de l'aluminium. Ces liquides sont corrosifs et difficiles à manipuler. Avec un système de chauffage par laser associé à un creuset étanche, nous avons étudié différentes compositions du système NaF–AlF_3–Al par RMN de ^{27}Al, ^{23}Na et ^{19}F in situ, à 1030°C. Les échantillons ont ensuite été caractérisés, après refroidissement à température ambiante, par RMN MAS, diffraction des rayons X et microscopie, afin de décrire la structure des phases solidifiées. ***Pour citer cet article : I. Nuta et al., C. R. Chimie 7 (2004).***

Keywords: ^{27}Al; ^{23}Na; ^{19}F; High-temperature NMR; Aluminium electrolysis; NaF–AlF_3–Al,

Mots clés : ^{27}Al ; ^{23}Na ; ^{19}F ; RMN haute température ; Électrolyse de l'aluminium ; NaF–AlF_3–Al

1. Introduction

In the Hall–Heroult electrolytic process used for the production of aluminium, the electrolyte consists of a complex mixture of AlF_3, Al_2O_3, LiF, NaF, and CaF_2. In the industrial cells, the metal produced has a higher density than the bath and falls down at the bottom of the cell. The metal is then in contact with the electrolyte and the graphite container. It can induce secondary reactions, such as aluminium dissolution in the bath, which will influence strongly the electrical rate of the process [1]. Solubility of aluminium is low (≈ 0.1 wt% Al) and depends on different factors, such as the acid-

* Corresponding author.
E-mail address: nuta@cnrs-orleans.fr (I. Nuta).

doi:10.1016/j.crci.2003.12.015

Table 1
Typical acquisition conditions used for high-temperature NMR experiments

Nucleus	Frequency (MHz) (9.4 T)	Number of scans	Pulse length (μs)	Recycle delay (s)	Reference
^{19}F	376.3	8	18	5	$CFCl_3$ 1 M
^{27}Al	104.2	64	20	0.25	$Al(NO_3)_3$ 1 M
^{23}Na	105.8	32	30	0.5	NaCl 1 M

ity of the melt, the temperature and the nature of additives. Compared to the other metals-molten salts systems, the system Al–NaF–AlF_3 is considerably more complex. In addition to the Al dissolution in the salt, one must take into account exchange reactions such as $Al + 3\,NaF \leftrightarrows AlF_3 + Na$, and the appearance of new species. The sodium metal arising from the reduction of Al becomes the major component of the vapour phase over the melt and induces also a number of secondary reactions. Fog formation and Al droplets dispersed within the melt also contributes to the concentration of dissolved metal. Visual observations, analysis of the metal in the quenched sample, weight loss and vapour pressure measurements are reported in the literature [1–7] and give some idea of the complexity characterizing that system.

These liquids are corrosive, hygroscopic, and difficult to study experimentally. We have recently reported a multinuclear (^{27}Al, ^{23}Na, and ^{19}F) study of the high-temperature binary NaF–AlF_3 liquids, using the laser-heated NMR set-up developed in Orléans [8]. The chemical shifts evolutions coincided rather well with the existence of AlF_4^-, AlF_5^{2-}, and AlF_6^{3-} complexes in melts, with proportions depending on the composition. For compositions between cryolite and chiolite ($0.25 > X(AlF_3) > 0.38$), an average coordination of five has been proved to explain the NMR and Raman [9] data obtained in these systems. In the present study, we use the same heating device and try to characterize by in situ high-temperature NMR the structural modifications caused by aluminium interaction with the molten electrolyte. In situ ^{27}Al, ^{23}Na and ^{19}F Nuclear Magnetic Resonance spectra were obtained for different compositions of the NaF–AlF_3–Al system in the temperature range between 800 and 1030 °C, and compared with those obtained for the same compositions, but without aluminium. The direct observations of structural modifications in the melts at high temperature, or during cooling, are combined to room-temperature characterizations of the solidified samples by MAS NMR, X-ray diffraction and microscopy. The use of different techniques helps to further constrain models of the aluminium action in cryolitic melts.

2. Experimental

Compositions ranging from 14 to 50 mol% AlF_3 were prepared by mixing suitable amounts of dried NaF and AlF_3 powders. The aluminium metal of high purity (Péchiney) is then introduced as small pieces (~2 to 3 mg). For the cryolite composition (25 mol% AlF_3), we have used pure natural cryolite from Greenland. All preparations have been made in a glove box under dry argon. 50 to 70 mg was put in a BN crucible tightly closed with a screw cup.

The high-temperature NMR experiments have been acquired using the previously described high-temperature laser-heated system developed at the CRMHT Orléans (France) [8,10]. A boron nitride crucible is directly heated by a continuous CO_2 laser ($\lambda = 10.6$ μm). The RF coil is thermally isolated by a ceramic shield and cooled by a simple airflow at room temperature.

All NMR experiments have been carried out using a Bruker DSX400 NMR spectrometer operating at 9.4 T. The NMR spectra have been acquired using single-pulse excitation and typical acquisition conditions are reported in Table 1. ^{27}Al, ^{23}Na, and ^{19}F chemical shifts are referenced to 1-M aqueous solutions $Al(NO_3)_3$, NaCl and $CFCl_3$, respectively, at room temperature, and are accurate to ±0.5 ppm. Samples are heated directly in the liquid, 10 °C above their melting point, and spectra are registered every 5 min in the melt to follow the sample's evolution.

^{27}Al, ^{23}Na and ^{19}F solid-state MAS NMR spectra have been obtained at room temperature on quenched samples after HT NMR experiments. The solid-state NMR data were collected with the same spectrometer (9.4 T), using a 2.5-mm MAS probe for a 35-kHz spinning rate. The acquisition parameters were chosen to optimise the resolution: short pulse lengths (0.5 μs),

recycle times of 1 to 5 s and high number of scans (1024).

The XRD powders patterns were collected at room temperature on a Philips PW1729 diffractometer (CuKα radiation). The pictures in Fig. 4 have been obtained with an Environmental Electron Scanning Microscope (ESEM) PHILIPS TMP XL 40. Compared to a conventional SEM, ESEM offers the advantages of samples observation under controlled atmosphere and without any prior conductive coating.

3. Results and discussion

The high-temperature NMR spectra for ^{27}Al, ^{19}F and ^{23}Na consist in a single Lorentzian line, characteristic of rapid exchange between the different species in the liquid. The peak positions represent the weighted averaged chemical shifts. The chemical shifts values that we have already reported in solid and molten fluoroaluminates [10], can help us to correlate the evolutions observed on spectra with structural modifications in the melt.

We have reported in Fig. 1 ^{27}Al spectra of some selected compositions, heated 10 °C above their melting point and showing the spectral evolution when aluminium is added.

Up to 37 mol% AlF_3, corresponding to the chiolite ($Na_5Al_3F_{14}$) composition, the peaks are systematically shifted towards higher chemical shifts values. Most significant changes are observed for aluminium and fluorine nuclei, while the ^{23}Na chemical shifts measured coincide rather well with values obtained for the corresponding compositions without metal. For higher AlF_3 contents, the position of the line is not modified by aluminium addition. It confirms the influence of the composition on the aluminium solubility in the molten NaF–AlF3 system [2].

The line is also slightly enlarged, with linewidths of 350–400 Hz for ^{27}Al, compared to 100–150 Hz without metal. This broadening, observed for the different nuclei, can be associated to the paramagnetic influence of metallic dispersions in the melt, while the shifts observed only for ^{27}Al and ^{19}F signals can be attributed to a modification of the species distribution. By comparison with the data obtained for compositions without metal, it would correspond to a lower average coordination. In Fig. 1, the evolution of the ^{27}Al spectra shows that the system reaches pseudo-equilibrium after 15 min, typically. We have limited the heating duration to 20 min. It seemed to be enough to reach a 'stable' state, as it can be expressed by the constant position of the line. Nevertheless, we have noticed after the NMR experiments some vapour deposit on the lid. Some fog-like streams have already been described in the literature and have been attributed to sodium

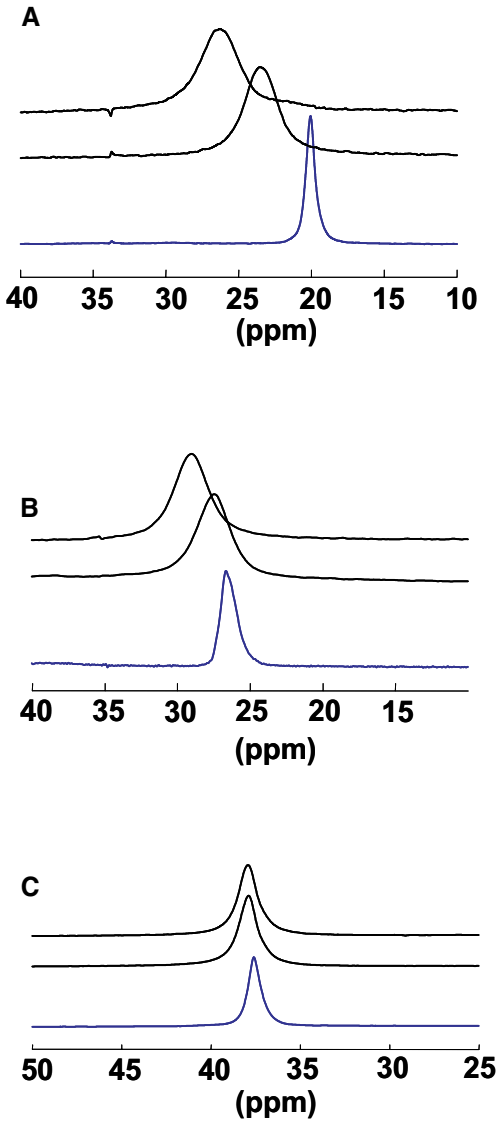

Fig. 1. ^{27}Al HT spectra of 28 mol% (a), 37 mol% (b) and 46 mol% AlF_3(c) compositions. The lower spectrum (in blue) corresponds to the composition without Al and the two upper spectra with aluminium, after heating 15 and 20 minutes up to the stabilization of the signal.

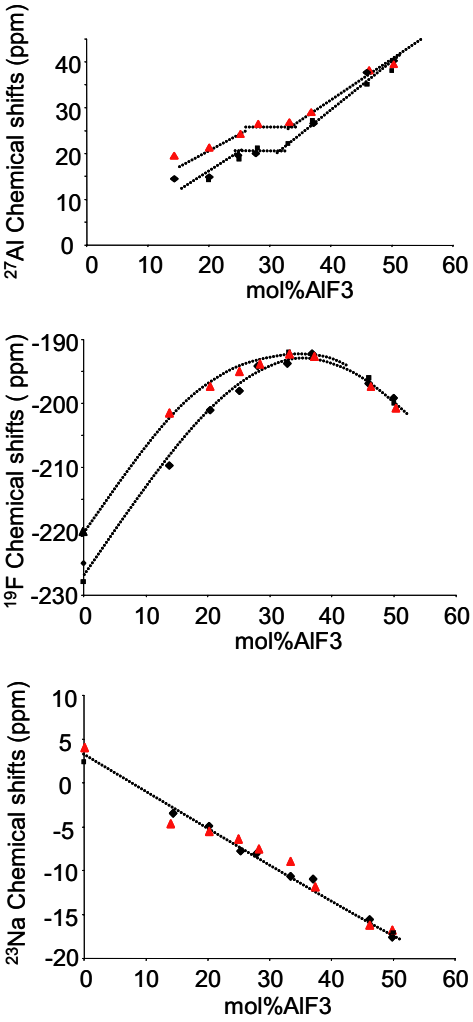

Fig. 2. ^{27}Al, ^{19}F and ^{23}Na chemical shifts evolution with composition. Comparison between the values measured with (▲) and without (◆) Al (this work); ■: [10].

vapours [1,11]. These vapours would arise from the reaction of aluminium with the melt and becomes denser in NaF-rich melts. The shifts observed for ^{27}Al and ^{19}F signals could then be associated with NaF loss and thus enrichment of the mixture in AlF_3.

We have reported in Fig. 2 the evolution of the ^{27}Al, ^{19}F, and ^{23}Na chemical shits measured in the melt for the different NaF–AlF_3 compositions with and without Al metal additions.

For the compositions without metal, as it has been already reported by Lacassagne et al. [8], going from NaF to AlF_3, we observe a continuous increase of $\delta_{^{27}Al}$. Some peculiar evolution is observed between 25 and 37 mol% AlF_3, where the ^{27}Al a chemical shift shows a plateau corresponding to average five fold coordination. For ^{19}F, the chemical shifts values grow from NaF to a maximum in the same range of composition (~194 ppm), and lowers for higher contents of AlF_3. In both cases, we notice a slope change between the compositions of cryolite, Na_3AlF_6 (25 mol%AlF_3) and chiolite, $Na_5Al_3F_{14}$ (37 mol% AlF_3). When aluminium is added, we observed a clear increase in the chemical shifts for NaF-rich melts, i.e. for compositions lower than 37 mol%AlF_3. The values measured are systematically higher. It is known that the NaF/AlF_3 ratio influences the solubility of metallic aluminium in molten cryolite melts. Different dissolution models have been proposed, suggesting the formation of fluoroaluminate species with lower coordination [1]. These species, if they could be detected, should have a higher chemical shift compared to the AlF_4^- at 38 ppm [8].

The chemical shifts experimentally measured in NaF–AlF_3 melts with aluminium addition, expressed this structural evolution by means of an averaged value systematically higher than that measured in the aluminium-free system.

In order to characterize the phases formed in the melt, we have combined this in situ approach with the characterization of the solidified samples at room temperature, by different techniques. Up to the cryolite composition (25 mol% AlF_3) with 3 mg aluminium added, the XRD pattern of the solidified melt is explained as a mixture of NaF, cryolite, and chiolite. According to the phase diagram [12], only cryolite should be formed in that range of composition. The presence of chiolite agrees well with the AlF_3 enrichment of the melt. This result is confirmed by MAS NMR. The ^{27}Al, ^{23}Na, and ^{19}F MAS spectra show the presence of a non-negligible proportion of chiolite, even for low AlF_3 content. We show in Fig. 3 the characteristic ^{23}Na and ^{19}F spectra, for the 14- and 25-mol% AlF_3 solidified compositions. The ^{23}Na spectra correspond mainly to the cryolite signature, with two components at –1 (C_Q = 1.1 MHz) and –12 ppm (C_Q = 1.4 MHz) [10]. The signal of chiolite is also visible and characterized by two distinct signals at –7 and –21 ppm. These signals are broad and characteristic of large quadrupolar interaction, 3.2 and 1.5 MHz respectively [13]. We have reported in the upper frame (Fig. 3) the decomposition of the experimental spectrum, showing each individual component.

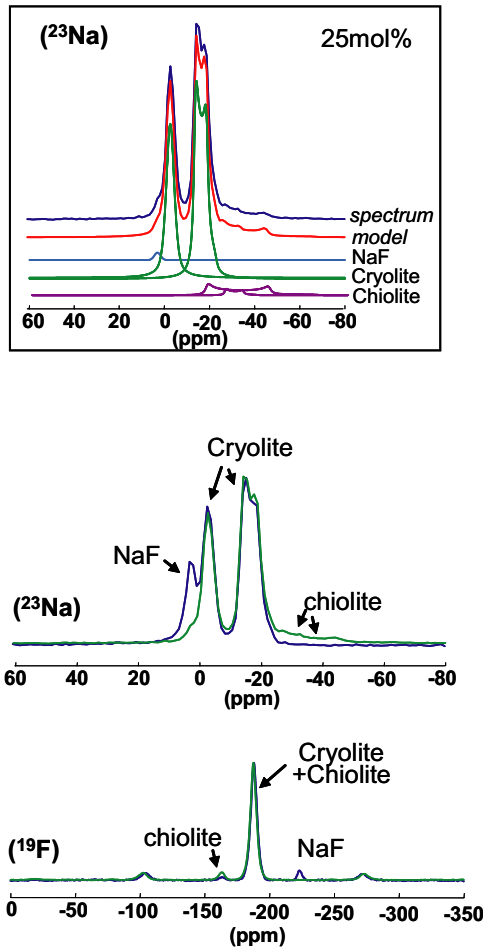

Fig. 3. ^{23}Na and ^{19}F MAS NMR spectra of 14-mol% (blue) and 25-mol% (green) solidified melts. In the upper frame, we report the 25-mol% ^{23}Na experimental and modelled spectra, showing the different components of the signal.

The presence of chiolite is more clearly detectable in the ^{19}F MAS NMR spectrum. The ^{19}F spectra of cryolite and chiolite phases differ only by a small line at –162 ppm for the chiolite, while the chemical shifts of the other F atoms are very closed and cannot be separated in our experiments.

In order to better describe to microstructure of such solidified systems, we have reported in Fig. 4 ESEM micrographs of the cryolite composition with aluminium metal (3 mg) added. In this picture, we have selected a well-defined area where we can evidence dispersions of small metallic particles, with size ranging between 1 to 3 μm. The X-ray mapping in Fig. 4b shows more clearly the Al repartition. In another part

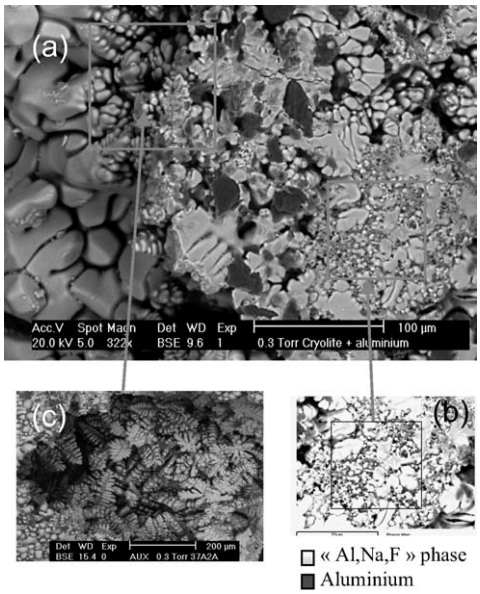

Fig. 4. (**a**) ESEM micrograph and (**b**) X-ray mapping of aluminium in a solidified melt of cryolite + aluminium after an NMR experiment. Comparison with (**c**) ESEM micrograph in solidified melt of chiolite + aluminium in the same conditions.

of the sample, we observed a microstructure identical to what is obtained for the reaction of the chiolite with aluminium metal as shown in Fig. 4c. This microstructure is not present in cryolite or chiolite samples without metal, and can be associated to a new AlF_3-rich phases.

4. Conclusion

The high-temperature NMR experiments have shown the evolution of the melts with aluminium dissolution. We have observed a systematic shift towards higher chemical shifts values for ^{27}Al and ^{19}F signals, attributed to the creation of new 'AlF_3' species with lower average coordination, while the ^{23}Na signals are just slightly modified.

The results obtained by MAS NMR, XRD, and ESEM techniques show the enrichment of the solidified samples by chiolite and seem to confirm the exchange reaction $3\,NaF + Al \leftrightarrow AlF_3 + 3\,Na$ reported in the literature [1].

Acknowledgements

The authors acknowledge Sylvie Bouvet from CRV-Pechiney for the aluminium samples. I.N. thanks the

CNRS and the 'Région Centre' (France) for financial support.

References

[1] J. Thonstad, P. Fellner, G.M. Haarberg, J. Hives, H. Kvande, A. Sterten, Aluminium Electrolysis, 3rd ed, Aluminium Verlag, Düsseldorf, Germany, 2001.
[2] R. Ødegård, A. Sterten, J. Thonstad, Light Metals (1987) 389.
[3] V. Danek, M. Chrenkova, A. Silny, Coord. Chem. Rev. 167 (1997) 1.
[4] H. Kvande, Light Metals (1980) 171.
[5] M.M. Vetyukov, V.B. Vinokurov, Non-Ferrous Metals 47 (6) (1974) 40.
[6] X. Wang, R.D. Peterson, N.E. Richards, Light Metals (1991) 323.
[7] R. Ødegård, Electrochim. Acta 33 (1988) 527.
[8] V. Lacassagne, C. Bessada, P. Florian, S. Bouvet, B. Ollivier, J.-P. Coutures, D. Massiot, J. Phys. Chem. B 106 (2002) 1862.
[9] V. Lacassagne, C. Bessada, D. Massiot, P. Florian, J.-P. Coutures, J. Chim. Phys. 95 (1998) 322.
[10] V. Lacassagne, C. Bessada, B. Ollivier, D. Massiot, P. Florian, J.-P. Coutures, C. R. Acad. Sci. Paris, Ser. IIb 325 (1997) 91.
[11] G.M. Haarberg, T. Støre, J. Thonstad, S. Pietrzyk, A. Silny, Al Symposium, Proceedings VIII, 25–27 September, Donovaly, Slovakia, 1995, pp. 79.
[12] J.-L. Holm, B.-J. Holm, Acta. Chem. Scand. 27 (1973) 1410.
[13] V. Lacassagne, P. Florian, V. Montouillout, C. Gervais, F. Babonneau, D. Massiot, Magn. Reson. Chem. 36 (1998) 956.